SCIENTIFIC REPORTS

OPEN

SUBJECT AREAS:
FUEL CELLS
BATTERIES
THERMOELECTRICS
SOLID-STATE CHEMISTRY

Received
28 September 2012

Accepted
14 December 2012

Published
24 January 2013

Correspondence and requests for materials should be addressed to Y.H.H. (huangyh@mail.hust.edu.cn) or Z.L.Z. (chm_zhangzl@ujn.edu.cn)

Evaluation of $Ca_3Co_2O_6$ as cathode material for high-performance solid-oxide fuel cell

Tao Wei[1], Yun-Hui Huang[1], Rui Zeng[1], Li-Xia Yuan[1], Xian-Luo Hu[1], Wu-Xing Zhang[1], Long Jiang[1], Jun-You Yang[1] & Zhao-Liang Zhang[2]

[1]State Key Laboratory of Material Processing and Die and Mould Technology, School of Materials Science and Engineering, Huazhong University of Science and Technology, Wuhan, Hubei 430074, China, [2]School of Chemistry and Chemical Engineering, University of Jinan, No. 106, Jiwei Road, Jinan 250022, China.

A cobalt-based thermoelectric compound $Ca_3Co_2O_6$ (CCO) has been developed as new cathode material with superior performance for intermediate-temperature (IT) solid-oxide fuel cell (SOFC). Systematic evaluation has been carried out. Measurement of thermal expansion coefficient (TEC), thermal-stress (σ) and interfacial shearing stress (τ) with the electrolyte show that CCO matches well with several commonly-used IT electrolytes. Maximum power density as high as 1.47 W cm^{-2} is attained at 800°C, and an additional thermoelectric voltage of 11.7 mV is detected. The superior electrochemical performance, thermoelectric effect, and comparable thermal and mechanical behaviors with the electrolytes make CCO to be a promising cathode material for SOFC.

Over the centuries, people always dream of applying the simple but powerful chemical equation, $H_2(g) + 1/2\ O_2(g) = H_2O(g)$ ($\Delta H_{727^\circ C} = -236.46$ kJ mol^{-1}), into the daily life[1–5]. Water is the only byproduct of the hydrogen-oxygen reaction. But so far, it is hopeful but difficult to have a hydrogen-powered future with clean ecological environment. The conventional solid-oxide fuel cells (SOFCs) with yttria-stabilized zirconia (YSZ) as electrolyte and hydrogen as fuel have showed excellent performance, which brings hope to us to provide clean energy at high temperature; but the electrochemical performance is highly susceptible to temperature[6–8]. Intermediate-temperature (IT) SOFCs have brought an extremely attractive prospect for low cost, high efficiency and mild operating condition[9]. For development of IT-SOFCs, cathode, anode and electrolyte materials are crucial. Compared with fast hydrogen oxidation reaction at the anode, oxygen reduction reaction (ORR) at the cathode is relatively slower. Therefore, exploration of new cathode materials with high performance has attracted much attention worldwide. Among them, the Co-based perovskites usually possess excellent electrochemical property as SOFC cathodes[10,11]. However, these cathodes such as $Ba_{0.5}Sr_{0.5}Co_{0.8}Fe_{0.2}O_3$ (BSCF) have some limitation. For example, they are sensitive to CO_2[12–14], and easy to encounter phase separation from cubic perovskite to mixture of cubic perovskite and hexagonal phase at temperatures below 850°C[15,16]. Moreover, compared with the IT electrolytes with low thermal expansion coefficient (TEC), such as $Ce_{0.8}Sm_{0.2}O_{2-\delta}$ (SDC) or $La_{0.8}Sr_{0.2}Ga_{0.8}Mg_{0.2}O_{3-\delta}$ (LSGM), the mismatched TEC and thermodynamic parameters restrict the long-term stability and economical competitiveness[17].

To be commercially viable, the IT-SOFC cathode materials need to overcome the barriers mentioned above. Substantial effort has been devoted to development of new cathode materials or innovation of cathode structures[18,19]. The new cathode materials should be stable in the cathode atmosphere and more catalytically active for oxygen reduction.

$Ca_3Co_2O_6$ (CCO) is an interesting compound, showing rich magnetic, electric and thermoelectric behaviors[20–24]. It consists of parallel one-dimensional (1D) $Co_2O_6^{6-}$ chains separated by Ca^{2+} ions, which is chemically stable up to 1300 K[25]. As a thermoelectric material, it is almost regarded as useless for application due to its high electrical resistivity at room temperature[26]. This may be the reason why few people research this compound as the thermoelectric material. However, in this work we use CCO in a totally different field, i.e., as a new cathode material for SOFC. We previously developed a thermoelectric SOFC concept by employing Co-based n-type $Na_{1-x}Cu_xCo_2O_4$ ($0 \le x \le 1$) as dual thermoelectric-cathode materials, and observed an additional thermoelectric voltage attached to the cell voltage[27]. Here we demonstrate $Ca_3Co_2O_6$ as the cathode material for IT-SOFC,

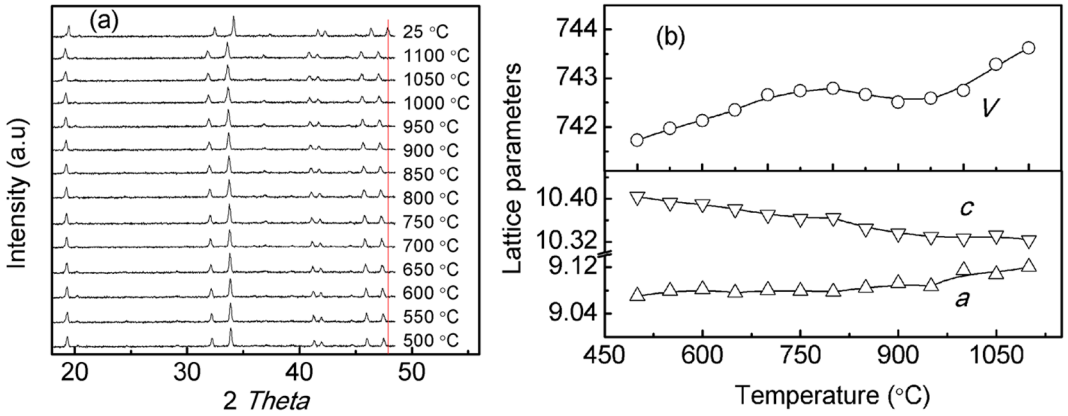

Figure 1 | (a) High temperature XRD patterns for $Ca_3Co_2O_6$ tested in air from 500 to 1100°C and finally at 25°C. (b) Dependence of temperature on lattice parameters a (Å), c (Å) and V (Å^3).

which exhibits high oxygen-reduction activity and excellent cell performance in air or oxygen atmosphere. Systematic evaluation on electrochemical performance as well as mechanical, thermal and thermoelectric behaviors has been carried out.

Results

Pure CCO can be obtained by sintering the precursor powder at 800–900°C for 10 h under air or oxygen atmosphere (Supplementary Fig. S1). The phase is indexed into a rhombohedral symmetry with space group R-3c[28]. To test the stability of CCO in the working atmosphere of SOFC cathode, high temperature X-ray diffraction (XRD) measurement was carried out in air from 500 to 1100°C. No decomposition was detected for CCO even at 1100°C (Fig. 1a), indicating that CCO is thermally stable. The diffraction angle shifts regularly with temperature (T). The calculated lattice parameters are shown in Fig. 1b. With increasing T, the axis a and unit cell volume V both increase, while the axis c decreases. The cell volume slightly expands at high temperature.

With CCO (20 μm thickness) as cathode, the electrochemical performance was investigated in a conventional dual chamber fuel cell with LSGM (100 μm thickness) as supporting electrolyte. 30 μm "NiO (40%) + SDC (60%)" layer served as anode, and 10 μm additional SDC layer as buffer interlayer between the anode and the electrolyte to prevent the interaction of NiO with LSGM. With air as oxygen source and H_2 as fuel, the maximum power density (P_{max}) reaches as high as 1.47 W cm^{-2} at 800°C, 1.14 W cm^{-2} at 750°C, and 0.66 W cm^{-2} at 700°C (Fig. 2). Such a high P_{max} indicates that CCO is a promising cathode material especially for IT-SOFC.

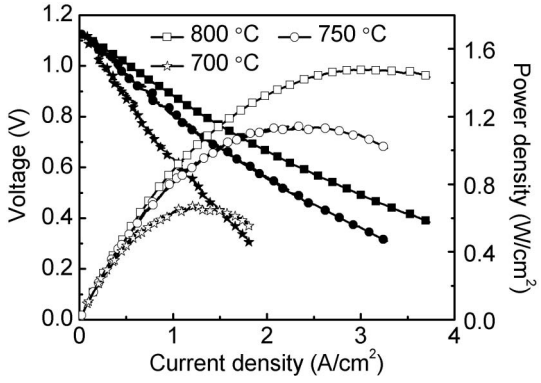

Figure 2 | **Electrochemical performance of the single cell voltage and power density as functions of current density obtained from Ni+SDC|SDC|LSGM (100 μm)|CCO dual-chamber fuel cell at different temperatures.**

In SOFC, the cathode provides reaction zone for oxygen reduction. Overpotential (η_c) is an important parameter to evaluate the cathode performance[1]. Here, we compared CCO with BSCF. The testing atmosphere for η_c was switched between air and pure oxygen. The η_c for CCO and BSCF cathode were tested first in air and then in pure oxygen with current densities from 0 to 1.6 A cm^{-2} at 800°C. As shown in Fig. 3, the η_c values are very low for both of the two cathodes. In air atmosphere, the η_c value of the CCO cathode is slightly higher than that of BSCF, but it drops obviously from 0.37 to 0.24 V when the atmosphere is switched from air to oxygen. If the testing atmosphere is switched back from oxygen to air, the η_c is recovered to the initial one for the two cathodes, demonstrating that both of them are stable. We define a parameter ξ to express the sensitivity of η_c on oxygen. ξ is calculated as $\xi = \text{slope}_{air}/\text{slope}_{oxygen}$ from the slope of η_c tested in air and oxygen. The ξ is 1.54 for CCO and 1.21 for BSCF. The higher ξ indicates that CCO is more sensitive than BSCF for oxygen catalyzing reaction as SOFC cathode.

Further evaluation was carried out for CCO as cathode in SOFC to match with several commonly-used IT-electrolytes. We tested the performances of the single cells supported by 300 μm thick LSGM, SDC and $BaZr_{0.1}Ce_{0.7}Y_{0.2}O_3$ (BZCY) electrolytes (Fig. 4). As expected, the cells show acceptable power density and stability. The P_{max} at 800°C is 0.76 W cm^{-2} for LSGM, 0.51 W cm^{-2} for SDC and 0.40 W cm^{-2} for BZCY. Obviously, with LSGM as electrolyte, the power output is the highest. For the sake of comparison with the CCO cathode, we fabricated 300 μm LSGM-supported single cell with "80% BSCF + 20% SDC" as cathode. Under exactly the same operating condition, the P_{max} at 800°C is 0.76 W cm^{-2} for CCO and 0.68 W cm^{-2} for "BSCF + SDC". The former exhibits higher power

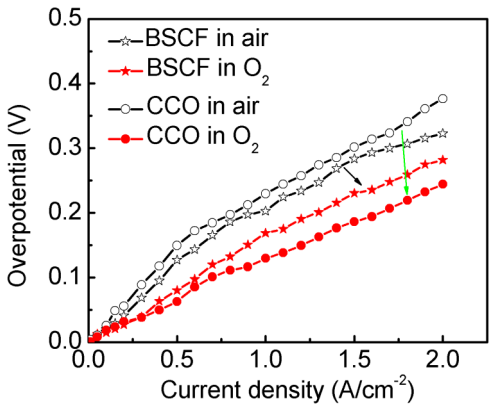

Figure 3 | **Overpotential η_c for CCO and BSCF cathodes as a function of current density operating in air and pure oxygen atmosphere at 800°C.**

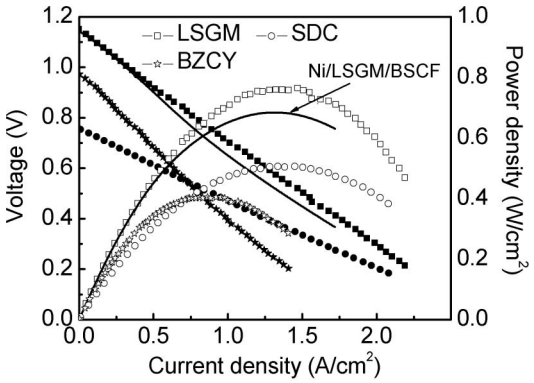

Figure 4 | Power densities for the single cells with CCO as cathode supported by different electrolytes (300 μm LSGM, SDC and BZCY). The cell Ni+SDC|SDC|LSGM(300 μm)|BSCF is taken as a comparison.

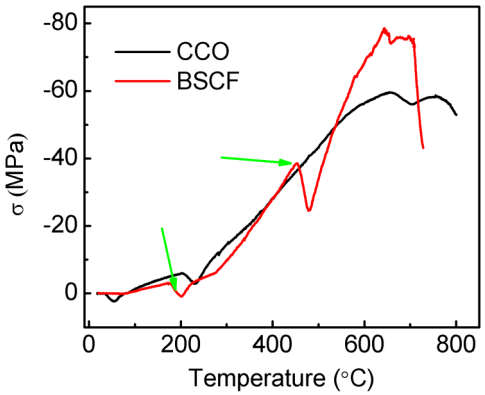

Figure 5 | Thermal stress σ as a function of temperature for CCO and BSCF.

output than the latter. Electrochemical impedance spectroscopy (EIS) of the LSGM-based single cells was measured under open current voltage (OCV) (Supplementary Fig. S2). Polarization resistance of the CCO cathode was measured on symmetric CCO|LSGM|CCO half cells. Area specific resistance (ASR) was determined from raw impedance plots. The ASR value is only 0.13 $\Omega\,cm^2$ for CCO at 800°C (Supplementary Fig. S3), which is comparable to some excellent cathode systems reported previously[29,30]. The low resistance may result in a low power loss due to ohmic drop. To confirm this, we further tested the stability of the 300 μm LSGM-supported CCO cell. The cell was operated with a preset voltage of 0.6 V for 100 h at 800°C. No obvious change in P_{max} was observed (Supplementary Fig. S4). After running the single cell for 100 h, no impurity was detected for the CCO cathode; and no chemical reaction took place between CCO and LSGM examined by XRD patterns (Supplementary Fig. S5), indicating that CCO is chemically stable in the working environment. The morphology of the tested cell was observed by scanning electron microscope (SEM, Fig. S6), indicating a close connection between CCO and LSGM. In addition, XRD testing also indicates no obvious chemical reaction between CCO and other IT-electrolytes (SDC and BZCY) (Fig. S7). The obtained high power density, long stable operation and chemical stability demonstrate that CCO is a promising cathode material to match the IT-electrolytes.

As cathode material, the comparability of thermal and mechanical behaviors with the electrolyte is significantly important especially for the large-scale planar or tubular type stacks. Thermal expansion coefficient (TEC) was measured. Since the Co-rich perovskites usually undergo a transition from low-spin to high-spin state with increasing temperature, their TECs are higher than those of LSGM and SDC electrolytes[17,31,32]. Mismatch in TEC will restrict the cobalt-based cathodes from practical application. For CCO, the linear thermal expansion is almost linearly dependent on temperature. Its TEC value is $(12.02 - 17.07) \times 10^{-6}\ K^{-1}$ in the temperature range from RT to 900°C (Supplementary Fig. S8), which matches well with the commonly-used IT-electrolytes. Compared with the electrolyte with low TEC, the cathode particles will be readily pressed out during heating due to large TEC (illustrated in Fig. S9). In fact, the extrusion process essentially comes from inner thermal-stress σ of the cathode particles. Therefore, σ is an ideal parameter to evaluate the cathode mechanical property. The σ of CCO and BSCF were tested with Gleeble 3500 System from RT to 800°C (Fig. S10). As shown in Fig. 5, with increasing T, BSCF and CCO both have a small abrupt change in σ at 200°C. This can be explained by flattening the porous Ag paste layer at about $\sigma = 3$ MPa. BSCF undergoes a great change in σ from 38.2 to 24.7 MPa at 450°C, which is mainly due to the partial damage of the column under high stress. For CCO, the column sample keeps stable without any damage or crack until 59.7 MPa at 657°C. With further increasing T, BSCF exhibits much higher σ caused by larger TEC, and is broken completely when $\sigma = 78.4$ MPa at 704°C; whereas CCO only shows a little damage even at 800°C. This means that CCO exhibits higher ability to bear deformation or cracking than BSCF as cathode during thermodynamic SOFC operation.

Under the working condition of SOFC, the cathode film must connect the electrolyte tightly to ensure rapid transport of oxygen ions in between them. The interfacial shearing stress τ is relatively intuitive to evaluate the match for the cathode film on the electrolyte surface. As shown in Figs. 6a and 6b, the τ value for CCO is much higher than that for BSCF. After testing, we observed that the whole BSCF cathode film separated from LSGM, whereas the CCO film still connected well with LSGM (Fig. 6c, d). The lower σ and higher τ values demonstrate that CCO can match better with LSGM than BSCF.

Discussion

In CCO, $CoO_{6/3}$ coplanar-sharing octahedra and $CoO_{6/3}$ polyhedra of trigonal prisms connect alternately to form subsystem chains, as illustrated in Fig. 7a. The subsystem chains array in a subparallel mode along the c axis. For the conventional Co-based perovskite cathode, the primary reaction zone for catalysis of oxygen reduction is the cobalt octahedra. We suggest that the primary zone in CCO cathode for oxygen diffusion, dissociative adsorption and charge transfer happen through the chains of coplanar-sharing octahedra and trigonal prisms (see the scheme in Fig. 7b).

Considering the low resistance (Fig. S3b), CCO should be a mixed oxide-ion/electron conductor (MIEC). Since it is chemically stable[25], the normal molecular formula is stoichiometric $Ca_3Co_2O_6$. We tested its thermal behavior in air from room temperature to 900°C to examine the possible oxygen vacancy. The thermogravimetric (TG) curve (Fig. S11) shows a clear weight loss of about 1.1% at 600–700°C, which should be ascribed to the oxygen escape from the lattice. The calculated oxygen vacancy concentration δ is 0.23 when the temperature is high than 700°C, i.e., CCO can be written as $Ca_3Co_2O_{5.77}$. Oxygen permeation property was further measured for the CCO film by gas chromatography (GC). The detected oxygen ionic conductivity is $9.5 \times 10^{-3}\ S\,cm^{-1}$ at 800°C. The yielded oxygen vacancy and considerable ionic conductivity confirm that CCO is indeed an MIEC, which can accelerate the electrochemical reaction by expanding the oxygen reduction reaction zone from three phase boundary to the whole cathode. The MIEC behavior of CCO can be attributed to its unique coplanar-sharing chain structure, which can provide a short distance for transportation of oxygen ions and electrons between octahedra and trigonal prisms. Moreover, it may produce three possible channels for oxygen ions and electrons transport from one $CoO_{6/3}$ structure to another with more convenient path (Fig. 7c). This can explain why CCO exhibits high power density and low overpotential as cathode material.

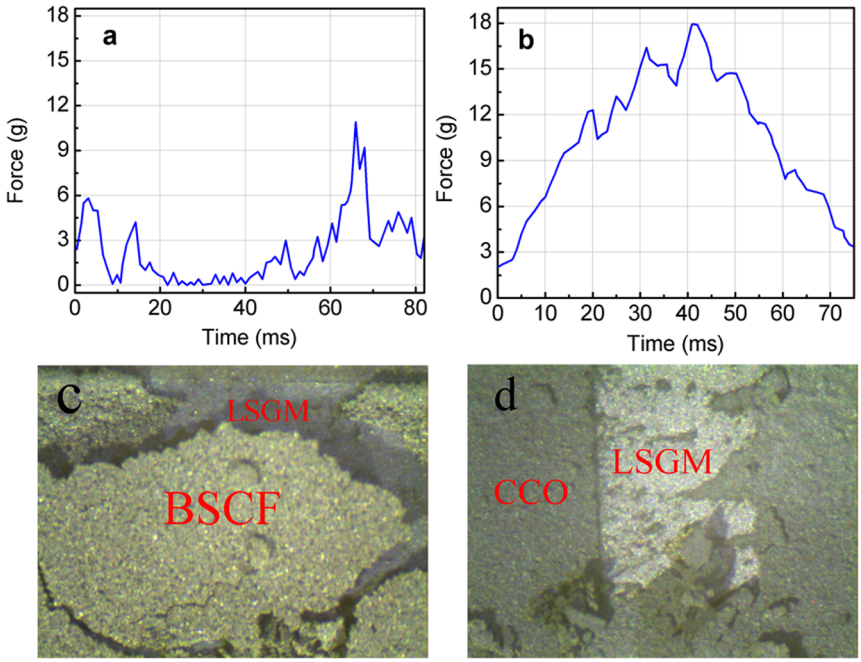

Figure 6 | The curves of interfacial shearing stress τ measured at room temperature for the celles with (a) BSCF cathode and (b) CCO cathode. The optical photoes after τ testing for the cells with (c) BSCF cathode and (d) CCO cathode.

Our experimental results of TEC, σ and τ show that CCO can thermally and mechanically match well with several IT-electrolytes, which also account for the stable power output. For practical application, cell local damage caused by high temperature gradient is a big challenge for the cell design and internal thermal management. In general, two routes can be employed to solve this problem. One is to remove the cell internal heat by increasing the air mass flow, but it will reduce the air utilization. The other is to enhance the cell operating voltage (for example, for the YSZ-based cell, the operating voltage is set at $\geq$ 0.7 V not at the peak power voltage 0.5 V), but this will result in reducing the valuable cell power density[33]. As described in our previous work[27], if the thermoelectric material is used as electrode for SOFC, it will not only transfer the heat to electricity to generate an additional voltage (ΔV), but also reduce the cell temperature gradient to a certain extent. Therefore, the thermoelectric component is helpful for the SOFC thermal transfer. The thermoelectric voltage can be expressed as $\Delta V = S*(T_1 - T_2)$, where S is the Seebeck coefficient and $(T_1 - T_2)$ is the temperature gradient. The generated ΔV can be attached to the cell voltage to increase the operation voltage of the cell. With the increase of furnace temperature, the power output of the thermoelectric SOFC will increase. CCO is a thermoelectric material, which shows a heat-to-electricity conversion over the IT-SOFC working temperature range (Supplementary Figs. S12, S13). The extra thermoelectric power was measured on a designed SOFC with elongated porous CCO column (1.5 cm in length and 1 cm in diameter) as cathode. The fabrication details of the thermoelectric SOFC was described elsewhere[27]. The thermoelectric SOFC was continuously monitored at 0.6 V for 1 h at 800°C. As shown in Fig. 8, compared with the preset 0.6 V testing voltage, the elongated CCO cathode creates additional 11.7 mV thermoelectric voltage by consuming the waste heat. In addition, the average open-circuit voltage (OCV) increases from 1.121 to 1.134 V due to the CCO thermoelectric cathode (Fig. S15). The created thermoelectric voltage monotonically increases with T from 700 to 800°C (Fig. S14). The results clearly confirm that the CCO cathode can produce additional thermoelectric voltage attached to the cell voltage, which favors not only the reduction of cell temperature gradient but also the enhancement of cell power output.

In summary, we developed a new Co-based cathode material for SOFC to attain superior performance. Systematic evaluation was carried out for $Ca_3Co_2O_6$ as the cathode material. Measurements of some important thermal and mechanical parameters TEC, σ

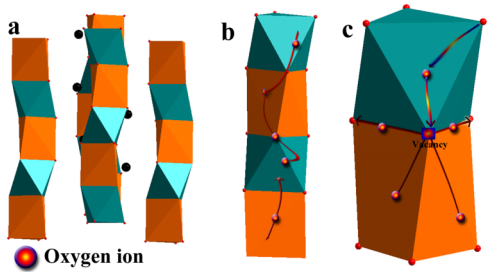

Figure 7 | (a) The CCO crystal structure with the $CoO_{6/3}$ coplanar-sharing octahedron and polyhedra of trigonal prisms form the subsystem chains. (b) The oxygen ions conduction diagram in CCO subsystem chain. (c) Three possible channels for oxygen ion and electron transport from one $CoO_{6/3}$ structure to another.

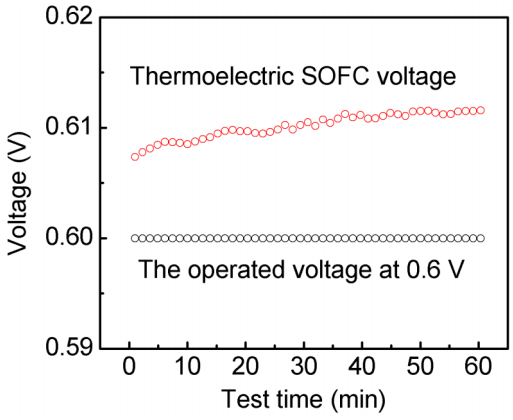

Figure 8 | **The generated thermoelectric voltage by convert the fuel cell waste heat to electricity with column CCO thermoelectric cathode.**

and τ show that CCO can match well with several commonly-used IT-electrolytes whatever LSGM, SDC or BZCY, which is promising for application without damage or chemical reaction over long cell operating period. Maximum power density as high as 1.47 W cm^{-2} and additional 11.7 mV thermoelectric voltage were obtained at 800°C, demonstrating that CCO is an excellent cathode material for IT-SOFCs. The superior electrochemical performance of CCO can be attributed to the mixed oxide-ion/electron conductive behavior caused by the unique coplanar-sharing chain structure, matched thermal and mechanical properties with the electrolyte and the thermoelectric effect. It should be pointed out that the generated power output from the thermoelectric effect in CCO may open up the possibility to promote the electrochemical performance by taking use of the waste heat in SOFCs.

Methods

Preparation of materials. The $Ca_3Co_2O_6$ (CCO) powders were synthesized via a sol-gel method. Citric acid was used as complexing agent. The molar ratio of citric acid to the total metal ions is 2 : 1. The process of preparation can be described as below. First citric acid was dissolved into distilled water, and then $Ca(NO_3)_2{\cdot}4H_2O$ and $C_4H_8CoO_4{\cdot}4H_2O$ were added respectively to achieve a clear solution. The solution was slowly evaporated on a hot plate under stirring over night to form a gel. The gel was decomposed at 250°C in air for 5 h to combust carbonaceous components. Then the powder was ground in a mortar, and calcined under pure oxygen or air at 800–900°C for 10 h. The SDC and BZCY were synthesized by sol-gel process, and LSGM was synthesized by conventional solid-state reaction, as described elsewhere[5].

Fuel cell fabrication and test. The fuel cells with a conventional configuration of Ni-SDC|SDC|electrolyte|cathode were fabricated with dense LSGM, SDC or BZCY as supporting electrolytes. The diameter of electrolyte was about 1.3 cm for the conventional fuel cell and 2 cm for the elongated columned cathode fuel cell. A thin SDC buffer interlayer with thickness of about 10 μm was used to prevent chemical reaction between NiO and LSGM; the SDC slurry was screen-printed onto LSGM disk and sintered at 1300°C for 1 h in stagnant air. No buffer interlayer was used for SDC and BZCY electrolyte. The anode layer (~30 μm) was attained by screen-printing the "NiO + SDC" (weight ratio of 60 : 40) slurry on the electrolyte and successively baking at 1250°C for 4 h. CCO slurry was screen-printed onto another side of the electrolyte and fired at 900°C for 5 h to achieve porous CCO cathode with thickness of ~20 μm and active area of 0.24 cm^2. "BSCF + SDC" (weight ratio of 80 : 20) cathode was fired at 1050°C for 2 h. Ag slurry and Ag wire were used as current collector for both the anode and cathode sides for electrochemical test. Ag has a high conductivity and cannot chemically react with CCO as confirmed by the XRD pattern (Fig. S16). Moreover, Ag has been proved to have a low electrochemical performance as cathode for oxygen catalyst[10]. Therefore, Ag current collector has almost no influence for the measured electrochemical data of CCO. For the testing cells, each one was sealed on an alumina tube with Ag slurry as sealing material and heated to 800°C. Pure H_2 was used as fuel to the anode; the cathode side was exposed into air. For evaluation of polarization performance for the CCO and BSCF cathodes in air or pure oxygen, half cells were placed in a half-open alumina tube reactor and then purged with the testing atmosphere before measurement.

Other characterizations. The phase purity and the structure parameters of the samples were checked by XRD with the Philips X'Pert PRO diffractometer by using filtered Cu K_α radiation. Power output and overpotential for the cells were measured in a vertical tubular furnace with PARSTAT 2273 electrochemical workstation. The morphology of the cells was observed by SEM (Sirion 200, Holland). TG curve for CCO was recorded from room temperature to 900°C in air on a Perkin-Elemer thermal analyser. Oxygen permeation property was measured by gas chromatography using a high temperature oxygen permeation apparatus. TEC was measured with a dilatometer (Linseis L75H, Germany) on the rod-shape samples (2 cm in length) with a relative density of >90% in air. Thermal stress factor σ was tested on the Gleeble 3500 system (DSI, US). For σ testing, the CCO and BSCF samples were made to dense columns with 14 mm in length and 10 mm in diameter. By applying current to the dense columns, the temperature of the column samples increased automatically due to self heating. A thin Ag layer was coated on the column to improve the conductivity. The improved conductivity (CCO column + Ag) is helpful to control the applied current density and hence the temperature rising rate. The interfacial shearing stress τ of CCO and BSCF thin film cathodes with LSGM electrolyte were tested with Dage 4000 bond tester (Nordson Company) at room temperature.

1. Barnett, S. A. *Handbook of fuel cell technology* (Wiley, Hoboken, NJ, 2003).
2. Barbir, F. *PEM fuel cells theory and practice* (Elsevier Academic Press, Burlington, MA, 2005).
3. Steel, B. C. H. & Heinzel, A. Materials for fuel-cell technologies. *Nature* **414**, 345–352 (2001).
4. Flytzani-Stephanopoulos, M., Sakbodin, M. & Wang, Z. Regenerative adsorption and removal of H_2S from hot fuel gas streams by rare earth oxides. *Science* **312**, 1508–1510 (2006).
5. Huang, Y. H., Dass, R. I., Xing, Z. L. & Goodenough, J. B. Double perovskites as anode materials for solid-oxide fuel cells. *Science* **312**, 254–257 (2006).
6. Robert, F. New tigers in the fuel cell tank. *Science* **288**, 1955–1957 (2000).
7. Co, A. C., Xia, S. J. & Birss, V. I. A kinetic study of the oxygen reduction reaction at $LaSrMnO_3$-YSZ composite electrodes. *J. Electrochem. Soc.* **152(3)**, A570–A576 (2005).
8. Zhou, X. B. *et al.* Performance of the single-chamber solid oxide fuel cell with a $La_{0.75}Sr_{0.25}Cr_{0.5}Mn_{0.5}O_{3-\delta}$ based perovskite anode. *J. Electrochem. Soc.* **157(5)**, B691–B696 (2010).
9. Wachsman, E. D. & Lee, K. T. Lowering the temperature of solid oxide fuel cells. *Science* **334**, 935–939 (2011).
10. Shao, Z. P. & Haile, S. M. A high-performance cathode for the next generation of solid-oxide fuel cells. *Nature* **431**, 170–173 (2004).
11. De Souza, R. A. & Kilner, J. A. Oxygen transport in $La_{1-x}Sr_xMn_{1-y}Co_yO_{3\pm\delta}$ perovskites Part I. Oxygen tracer diffusion. *Solid State Ionics* **106**, 175–187 (1998).
12. Arnold, M., Wang, H. H. & Feldhoff, A. Influence of CO_2 on the oxygen permeation performance and the microstructure of perovskite-type $(Ba_{0.5}Sr_{0.5})(Co_{0.8}Fe_{0.2})O_{3-\delta}$ membranes. *J. Membr. Sci.* **293**, 44–52 (2007).
13. Yan, A., Cheng, M., Dong, Y., Yang, W., Maragou, V., Song, S. & Tsiakaras, P. Investigation of a $Ba_{0.5}Sr_{0.5}Co_{0.8}Fe_{0.2}O_{3-\delta}$ based cathode IT-SOFC I. The effect of CO_2 on the cell performance. *Appl. Catal. B.* **66**, 64–71 (2006).
14. Yan, A., Maragou, V., Arico, A., Cheng, M. & Tsiakaras, P. Investigation of a $Ba_{0.5}Sr_{0.5}Co_{0.8}Fe_{0.2}O_{3-\delta}$ based cathode SOFC: II. The effect of CO_2 on the chemical stability. *Appl. Catal. B.* **76**, 320–327 (2007).
15. Svarcova, S., Wiik, K., Tolchard, J., Bouwmeester, H. J. M. & Grande, T. Structural instability ofcubic perovskite $Ba_xSr_{1-x}Co_{1-y}Fe_yO_{3-\delta}$. *Solid State Ionics* **178**, 1787–1791 (2008).
16. Mueller, D. N., De Souza, R. A., Weirich, T. E., Roehrens, D., Mayer, J. & Martin, M. A kinetic study of the decomposition of the cubic perovskite-type oxide $Ba_xSr_{1-x}Co_{0.8}Fe_{0.2}O_{3-\delta}$ (BSCF) (x = 0.1 and 0.5). *Phys. Chem. Chem. Phys.* **12**, 10320–10328 (2010).
17. Ullmann, H., Trofimenko, N., Tietz, F., Stöver, D., Ahmad-Khanlou, A. Correlation between thermal expansion and oxide ion transport in mixed conducting perovskite-type oxides for SOFC cathodes. *Solid State Ionics* **138**, 79–90 (2000).
18. Molenda, J., Świerczek, K. & Zając, W. Functional materials for the IT-SOFC. *J. Power Sources* **173**, 657–670 (2007).
19. Han, D., Liu, X., Zeng, F., Qian, J., Wu, T. & Zhan, Z. A micro-nano porous oxide hybrid for efficient oxygen reduction in reduced-temperature solid oxide fuel cells. *Sci. Rep.* **2**, 462 (2012).
20. Aasland, S, Fjellvåg, H. & Hauback, B. Magnetic properties of the one-dimensional $Ca_3Co_2O_6$. *Solid State Commun.* **101**, 187–192 (1997).
21. Agrestini, S, Fleck, C. L, Chapon, L. C., Mazzoli, C., Bombardi, A., Lees, M. R. & Petrenko, O. A. Slow magnetic order-order transition in the spin chain antiferromagnet $Ca_3Co_2O_6$. *Phys. Rev. Lett.* **106**, 197204-1–197204-4 (2011).
22. Kamiya, Y. & Batista, C. D. Formation of Magnetic Microphases in $Ca_3Co_2O_6$. *Phys. Rev. Lett.* **109**, 067204-1–067204-5 (2012).
23. Mikami, M., Funahashi, R., Yoshimura, M., Mori, Y. & Sasaki, T. High-temperature thermoelectric properties of single-crystal $Ca_3Co_2O_6$. *J. Appl. Phys.* **94**, 6579–6582 (2003).
24. Mikami, M. & Funahashi, R. The effect of element substitution on high-temperature thermoelectric properties of $Ca_3Co_2O_6$ compounds. *J. Solid State Chem.* **178**, 1670–1674 (2005).
25. Brisi, C. & Rolando, P. The calcium oxide-cobalt (II) oxide-oxygen system. *Ann Chim (Rome)* **58**, 676–683 (1968).
26. Raquet, B., Baibich, M. N., Broto, J. M., Rakoto, H., Lambert, S. & Maignan, A. Hopping conductivity in one-dimensional $Ca_3Co_2O_6$ single crystals. *Phys. Rev. B* **65**, 104442-1–104442-6 (2002).
27. Wei, T., Huang, Y. H., Zhang, Q., Yuan, L. X., Yang, J. Y., Sun, Y. M., Hu, X. L., Zhang, W. X. & Goodenough, J. B. Thermoelectric solid-oxide fuel cells with extra power conversion from waste heat. *Chem. Mater.* **24**, 1401–1403 (2012).
28. Hervoches, C. H., Okamoto, H., Kjekshus, A., Fjellvåg, H. & Hauback, B. C. Crystal structure and magnetic properties of the solid-solution phase $Ca_3Co_{2-v}Mn_vO_6$. *J. Solid State Chem.* **182**, 331–338 (2009).
29. Liu, Q., Dong, X. H., Xiao, G. L., Zhao, F. & Chen, F. L. A novel electrode material for symmetrical SOFCs. *Adv. Mater.* **22**, 5478–5482 (2010).
30. Ralph, J. M., Rossignol, C. & Kumar, R. Cathode materials for reduced-temperature SOFCs. *J. Electrochem. Soc.* **150**, A1518–A1522 (2003).
31. Zeng, P., Chen, Z., Zhou, W., Gu, H., Shao, Z. & Liu, S. Re-evaluation of $Ba_{0.5}Sr_{0.5}Co_{0.8}Fe_{0.2}O_{3-\delta}$ perovskite as oxygen semi-permeable membrane. *J. Membr. Sci.* **291**, 148–156 (2007).
32. Feng, M. & Goodenough, J. B. A superior oxide-ion electrolyte. *Eur. J. Solid State Inorg. Chem.* **31**, 663–672 (1994).
33. Minh, N. Q. Ceramic fuel cells. *J. Am. Ceram. Soc.* **76**, 563–588 (1993).

Acknowledgements

We thank the Natural Science Foundation of China (Grant Nos. 50825203 and 21077043) and the PCSIRT (Program for Changjiang Scholars and Innovative Research Team in University, grant No. IRT1014) for support of this work.

Author contributions

T.W., Y.H.H., R.Z., L.X.Y., X.L.H. and W.X.Z. conceived and designed the experiments. T.W., Y.H. H. and Z.L.Z. analysed the measurements. T.W., L.J. and R.Z. prepared the experimental samples. T. W. and J. Y. Y. performed the thermoelectric testing. T. W. and Y. H. H. wrote the manuscript in collaboration with all the authors. We thank Prof. Zongping Shao and Mr. Dong Xu in Nanjing University of technology for oxygen permeation property measurement.

Additional information

Supplementary information accompanies this paper at http://www.nature.com/scientificreports

Competing financial interests: The authors declare no competing financial interests.

How to cite this article: Wei, T. *et al.* Evaluation of $Ca_3Co_2O_6$ as cathode material for high-performance solid-oxide fuel cell. *Sci. Rep.* **3**, 1125; DOI:10.1038/srep01125 (2013).